PLASMA SHEATH EFFECTS AND VOLTAGE DISTRIBUTIONS OF LARGE HIGH-POWER SATELLITE SOLAR ARRAYS

Lee W. Parker
Lee W. Parker, Inc.

SUMMARY

Knowledge of the floating voltage configuration of a large array in orbit is needed in order to estimate various plasma-interaction effects. The equilibrium configuration of array voltages relative to space depends on the sheath structure. The latter dependence for an exposed array is examined in the light of two finite-sheath effects neglected in previous analyses which have assumed the planar approximation based on the thin-sheath limit. One effect is that electron currents may be seriously underestimated. The other is that a potential barrier for electrons can occur, restricting electron currents. The problem is not a priori a thin-sheath problem either with respect to plasma electrons or with respect to wake effects. A conducting surface is assumed on the basis of a conductivity argument. Finite-sheath effects are investigated using the thick-sheath limit. The results of assuming thin-sheath and thick-sheath limits on the floating configuration of a linearly connected array are studied, under conditions appropriate to both LEO and GEO. Sheath thickness and parasitic power leakage are estimated analytically. Numerically computed fields using a 3-D code are displayed in the thick-sheath limit. Potential barriers appear in the cases of (a) a linearly connected array in GEO, and (b) an "overlapping sheath" interaction problem involving adjacent strips with large voltage jumps between them.

INTRODUCTION

High-power solar arrays for satellite power systems are presently being planned with dimensions of kilometers and with tens of kilovolts distributed over their surfaces. This paper is concerned with the "floating potential" of an array with exposed interconnects, that is, with the equilibrium voltage configuration under the conditions of (a) overall current balance, and (b) fixed relative voltages along the array between the positive and negative terminals. Knowledge of the floating configuration is needed for estimating a number of plasma-interaction effects, in both low earth orbit (LEO) and geosynchronous orbit (GEO). Among these are (a) parasitic power leakage due to ambient plasma currents, (b) power leakage due to ion thruster currents, (c) sputtering and erosion, (d) secondary-electron emission and cascade, (e) velocity wake effects, and (f) differential charging effects. The array will float so that a part of it is positive and the remainder is negative.

Two effects have been neglected in previous analyses. One of these is that the positive section may be smaller than the sheath thickness and may require a more general treatment than the usual planar approximation based on the thin-sheath limit. One result is that more electron current may be collected than may be expected on the basis of a thin sheath; this shortens the positive section further. Another effect is the possible appearance of a potential barrier for electrons (the array has a net negative charge); this tends to reduce electron currents, thus lengthening the positive section. The question can be decided only by self-consistent calculations including space charge. The problem is not really a thin-sheath problem a priori; the size of the positive section depends on the solution. Also, the thin-sheath concept must break down when the array is looking into its own wake.

In this paper we assume two limits, those of a thin sheath and a thick sheath, and calculate analytically the associated floating voltage configurations of a linear 40-kv array with exposed interconnects. The thick-sheath limit is useful for investigating finite-sheath effects. The true self-consistent solution may lie between the two limits. Potential barrier effects on the array voltages are neglected. The floating configurations can be determined more precisely including the effects of potential barriers by self-consistent numerical solutions (cf. ref. 1). Magnetic fields are neglected, as well as voltage drops due to internal currents.

Formulas and results obtained by analytical approximations for sheath thickness, and for parasitic power leakage in the two limits, are presented for both LEO and GEO. The structure of the sheath is computed using a 3-D computer code called PANEL (ref. 2), where a flat rectangular plate with a nonuniform distribution of surface voltage serves as a model for a flat high-voltage solar array. In the thick-sheath limit the field solution shows that the potential barrier for electrons has a height of 2 kv for a 40-kv array. Thus, for electrons with temperatures below 2 kev, the electron current would be reduced, and the positive section of the array would increase in size. The appearance of a potential barrier is typical in differential charging situations (refs. 1 and 3). PANEL was used also to compute fields for various finite sheath thicknesses, using a linearized space-charge model. The results (not shown here) indicate that the barrier decreases in height and approaches the edge of the array as the Debye length decreases.

Also examined is the "overlapping-sheath" question of current collection by adjacent areas with a large potential jump between them. (This could apply for example to exposed terminals on the back of an array.) The model consists of alternating strips at 0 and 1000 volts (assumed relative to space). The plasma currents are calculated using the "inside-out" method (ref. 4) of reversed trajectories. The high-voltage areas tend, through creation of potential barriers, to prevent the plasma particles repelled by them from reaching their low-voltage neighbor areas, thus controlling the current-voltage characteristics of the low-voltage areas.

CONDUCTIVITY OF INSULATED SURFACES

We assume here that the array has a conducting surface (interconnects exposed to the plasma). It should be noted that the alternative option of insulating the entire array from the plasma by a thin perfectly non-conducting dielectric coating is unfeasible, for the following reason. An insulated array would tend to float with all surface points equilibrated to a potential of the order of the plasma temperature (or of the photoelectron energy where photoemission is dominant). With large voltages (tens of kilovolts) existing on the array surfaces under the dielectric layer, a thin dielectric layer of the order of 20 microns thick can be subjected to electric fields E of the order of 10^7 v/cm, well above nominal breakdown thresholds. Hence breakdown is likely for very good insulators.

A small but finite dielectric conductivity, on the other hand, can change the problem essentially from that of an insulating surface to that of a conducting surface. To estimate the "cross-over" critical conductivity, we compare the rates of (a) surface discharging by conduction through the dielectric, and of (b) surface charging by plasma currents. The ratio of these rates may be approximated by $\sigma E/j$, where σ, E, and j denote the conductivity, internal electric field, and charging current density, respectively. This ratio should be greater than unity to avoid breakdown and effectively to provide conducting surfaces. Assuming $j=10^{-10}$ amp/cm^2 as typical of GEO conditions, and $E=10^6$ v/cm as a maximum allowed value, we obtain $\sigma E/j=10^{16}\ \sigma$(mho/cm). Hence $\sigma=10^{-16}$ mho/cm is the critical conductivity. A change in σ of a half of an order of magnitude in one direction or the other will make the layer essentially conducting or essentially nonconducting. Typical spacecraft insulating materials such as quartz, Kapton and Teflon have lower conductivities than this in the dark but higher conductivities than this in sunlight (ref. 5). Hence at least in sunlight a quartz- or Teflon-coated front surface may be considered conducting, and the analysis of this paper applies. (However, the Kapton backing presently contemplated for the back surfaces of the array is a good insulator in the dark and runs the hazard of incurring breakdowns.)

In the next section we treat sheath thickness, for the case where the sheath is due to the ambient plasma. Photoemitted or secondary-electron contributions should also be considered since in GEO they may contribute significantly not only to fluxes but also to space charge and reduced sheath thickness. Strong photoemission contributions are treated, for example, by Parker (ref. 6) and by Soop and by Schröder (see ref. 7). Their effects are also discussed briefly in the present paper.

SHEATH THICKNESS

We assume the solar array is a flat rectangular plate, with the voltage distribution on its surface varying linearly along one of the dimensions, and constant along the other dimension. The surface is assumed to be conducting (that is, the solar-cell interconnects are assumed to be exposed to the plasma). Figure 1 shows schematically how the sheath might look in a side view of the panel, with the floating voltages distributed from left to right. The negative

section on the left is relatively long, of length L_1. The positive section on the right is relatively short, of length L_2. The dividing point between the two sections is at space potential. The sheaths of the two sections are shown to thicken as the voltage relative to space increases in magnitude. The negative section (L_1) collects mostly ion current, while the positive section (L_2) collects mostly electron current. The linear voltage variation on the surface is shown in the lower part of the figure, going from negative V_1 at the most negative end to positive V_2 at the most positive end.

Sheath structures generally require self-consistent numerical solutions (e.g., refs. 1, 8-9). When the sheath is thin relative to the body dimensions, however, and consists essentially only of attracted ambient-plasma particles, an analytical approximation is available based on a "space-charge-limited" diode model, the so-called Child (or Child-Langmuir) model (ref. 10). This is a unipolar sheath model wherein the attracted charged particles are accelerated in a beam toward the collecting plate, starting with zero energy. If e and m denote the particle charge and mass, V denotes the voltage, j denotes the current density, and S denotes the diode plate separation, then the sheath thickness may be estimated from the Child law relating V, j, and S. In c.g.s. units, this is

$$S = (2e/m)^{1/4} \cdot V^{3/4}/(9\pi j)^{1/2} \qquad (1)$$

where the sheath thickness is identified with the plate separation. In sheath thickness estimations, it is customary to replace j by the random thermal current density at the sheath edge, $j_0 = en_0 (kT/2\pi m)^{\frac{1}{2}}$, where n_0 is the particle density and T is the temperature of the Maxwellian distribution. If there is also a significant drift velocity v_0 (as in the case of O^+ ions in LEO) toward the panel, j_0 may be replaced by $[\exp(-M^2) + \sqrt{\pi}\, M(1 + \text{erf } M)]\, j_0$, where M is the ion Mach number $M = (mv_0^2/2kT)^{\frac{1}{2}}$. Thus, in practical units, taking into account both thermal and drift (ion "ram") currents at the sheath edge, the planar equation (1) may be written

$$S(\text{meters}) = 9.33 \frac{V^{3/4}(\text{volts})}{n_0^{\frac{1}{2}}(\text{cm}^{-3}) \cdot T^{\frac{1}{4}}(\text{ev}) \cdot (\text{RAM})^{\frac{1}{2}}} \qquad (2)$$

where

$$\text{RAM} = \exp(-M^2) + \sqrt{\pi} M (1 + \text{erf} M) \qquad (3)$$

Equation 2 cannot be used when S is comparable with or exceeds the body dimensions. Corrections for non-planarity are frequently made using the analogous spherical diode model, where the particles move radially inward from an outer emitter to an inner spherical collector, with no angular momentum. Langmuir and Blodgett (ref. 11) give a table of factors which may be used in conjunction with equation (2). It should be noted that equation (2) assumes that the panel is looking into the ram direction and is invalid if the panel looks into the wake.

FLOATING CONFIGURATION BASED ON THIN SHEATH LIMIT

In the thin sheath limit, referring to figure 1 and assuming only attracted-particle contributions to the array currents (because of the large voltages compared with particle energies), and because in this limit the currents are constant over the two sections of the array, we may express the current balance condition as

$$RAM \cdot j_{io} \cdot L_1 = j_{eo} \cdot L_2 \tag{4}$$

where L_1 and L_2 denote, respectively, the lengths of the negative (left) and positive (right) sections; j_{io} and j_{eo} are the random thermal currents of ions and electrons, respectively; and RAM is defined by equation (3). If the array looks into the ram direction, RAM can be greater than unity for the ions. For equal ion and electron temperatures, equation (4) yields the ratio of the positive to negative lengths:

$$\frac{L_2}{L_1} = \sqrt{\frac{m_e}{m_i}} \cdot (RAM) \tag{5}$$

where m_e and m_i denote the electron and ion masses, respectively. Results for LEO and GEO are shown in table 1, under the columns labelled "THIN LEO" and "THIN GEO".

For LEO we assume oxygen ions with Mach number M=6.4 (ref. 12), which yields RAM=22.7. From equation (5) we obtain $L_2/L_1=0.132$, so that $L_2=117$ m is the length of the positive section of a one-kilometer array. Thus the positive end of a 40-kv array floats at $V_2=+4700$v. The negative section length and end voltage are $L_1=883$m and $V_1=-35300$v, respectively. These values of L_2, L_1, V_2, and V_1 are shown in the "THIN LEO" column of table 1. From equation (2), assuming in addition $n_0=10^5$ cm^{-3} and T=0.1 ev, we obtain sheath thicknesses $S_2=30$m and $S_1=28$m, as shown in table 1. Thus, the sheath is thin compared with the lengths of both the positive and negative sections. Hence the thin-sheath limit seems valid for LEO. However, it should be noted that we are neglecting edge effects and velocity-flow wake effects.

For GEO we assume hydrogen ions, with Mach number zero (i.e., RAM=1). From equation (5), we obtain $L_2/L_1=0.0233$. Hence the positive-section length and end-voltage of a one-kilometer 40-kv array are $L_2=23$m and $V_2=+900$v, respectively. The length and end-voltage of the negative section are $L_1=977$m and $V_1=-39100$v, respectively. These lengths and voltages are shown in the "Thin Sheath" diagram of figure 2. From equation (2), assuming $n_0=1$ cm^{-3} and T=10000ev, we obtain sheath thicknesses $S_2=150$m, that is, large compared with L_2; and $S_1=2600$m, that is, large compared with L_1. (See table 1.) Hence, the sheaths of both sections are thick rather than thin (even when the Langmuir-Blodgett spherical correction factors are applied), and the thin-sheath assumption in the absence and secondary and photoelectron contributions is invalid for GEO. However, since photoelectron and secondary-electron contributions are important in GEO, the sheath will be of finite thickness and its structure must be calculated

self-consistently (refs. 6 and 7). Nevertheless, the thick-sheath limit is useful for investigating finite-sheath effects.

FLOATING CONFIGURATION IN GEO BASED ON THICK SHEATH LIMIT

In the thick-sheath (Laplacian) limit, a sphere collects attracted-particle current density in accord with the well-known orbit-limited ideal Langmuir formula

$$j = \left(1 + c\frac{eV}{kT}\right) \cdot j_o \tag{6}$$

where j_o is the random thermal current density and c is equal to unity. Other 3-dimensional shapes as well can collect orbit-limited current in accord with equation (6) with c=1 (ref. 13). A flat circular surface (such as the end of a cylinder) has a linear current-voltage characteristic describable by equation (6) with c less than unity (ref. 14). We assume here that all points of the (conducting) solar-array surface collect current density proportional to $j_o V$. This implies that (a) the voltage everywhere is large such that eV/kT is large compared with unity, (b) only attracted particles contribute, (c) the coefficient c is the same for all points, and (d) there are no potential barriers. Then, since V=V(x) and j=j(x) are linear functions of position x on the panel surface, we must integrate j(x) over x to compute the total currents collected by the negative and positive sections. The current balance condition can be shown to yield

$$\frac{L_2}{L_1} = \left(\frac{m_e}{m_i}\right)^{1/4} \cdot (RAM)^{1/2} \tag{7}$$

for the ratio of lengths, independent of the coefficient c. That is, the thick-sheath ratio L_2/L_1 is the square root of the corresponding thin-sheath ratio in equation (5).

Results for GEO are shown in the last column of table 1, labelled "THICK GEO." The positive and negative sections of a one-kilometer array are L_2=132m and L_1=868m, respectively. The corresponding positive and negative end-voltages are V_2=+5300v and V_1=-34700v, respectively. These lengths and voltages are shown in the "THICK SHEATH" diagram of figure 2.

POWER LEAKAGE IN LEO AND GEO

We may estimate power losses to the plasma in a similar manner to that in which we estimated floating voltages above. For the thin-sheath limit, the current density is constant over the (positive or negative) section, and the voltage varies linearly. Hence the power density varies linearly. The average power loss per unit area may be shown to be given by

$$\bar{P}_{(\text{thin sheath})} = \frac{V/2}{\left[\frac{1}{j_{eo}} + \frac{1}{RAM \cdot j_{io}}\right]} \tag{8}$$

where V is the total voltage differential V_2-V_1 across the array and the other symbols have been defined above. In practical units, assuming Maxwellian distributions with equal ion and electron temperatures, the current density may be written

$$j_0(\text{amp/m}^2) = 2.68 \times 10^{-8}\, n_0(\text{cm}^{-3})\, \sqrt{T(\text{ev})/m(m_e)} \tag{9}$$

where $m(m_e)$ denotes the particle mass in units of the electron mass; and $\bar{P}$ becomes

$$\bar{P}_{(\text{thin sheath})}\left(\frac{\text{watt}}{\text{m}^2}\right) = 1.34 \times 10^{-8} \frac{V(\text{volts}) \cdot n_0(\text{cm}^{-3}) \cdot \sqrt{T(\text{ev})}}{[1 + \sqrt{m_i/m_e} \,/\, RAM]} \tag{10}$$

Again, the array is assumed to be looking into the ram direction in collecting ion currents, where RAM can be greater than unity. In LEO, assuming m_i/m_e= 29380, with values of n_0, T, and RAM given in table 1, and taking V=40000 volts, we obtain $\bar{P}\tilde{=}2$ watt/m^2. This value does not seem to represent a serious loss effect. It should be remembered, however, that the sheath could thicken, and power leakage could increase, near the edges and when the array looks into its own wake. In addition, we chose $n_0=10^5$ cm^{-3}; this value could go as high as 10^6 cm^{-3} in the F-region.

For the thick-sheath limit, the current density may be assumed to vary linearly, as was done for the floating configuration. Hence the power density varies quadratically. The average power loss per unit area may be shown to be given by

$$\bar{P}_{(\text{thick sheath})} = \frac{(cV/3)\cdot(eV/kT)}{\left[\frac{1}{\sqrt{j_{eo}}} + \frac{1}{\sqrt{RAM \cdot j_{io}}}\right]^2} \tag{11}$$

where c is the coefficient in equation (6). In practical units, $\bar{P}$ becomes

$$\bar{P}_{(\text{thick sheath})}\left(\frac{\text{watt}}{\text{m}^2}\right) = 0.89 \times 10^{-8} \frac{cV^2(\text{volts}) \cdot n_0(\text{cm}^{-3}) / \sqrt{T(\text{ev})}}{[1 + (m_i/m_e)^{1/4} \,/\, RAM^{1/2}]^2} \tag{12}$$

In GEO, assuming c=1, m_i/m_e=1836, the values of n_0, T, and RAM given in table 1, and taking V=40000 volts, we obtain $\bar{P}\tilde{=}0.0025$ watt/m^2, which seems inconsequential compared with about 100 watt/m^2 nominally deliverable by the solar cells.

On the other hand, if the array is in LEO and is looking into its own wake, so that the sheath is thick rather than thin, equation (12) yields $\bar{P}$=22700 watt/m^2, indicating that catastrophic power losses can occur. (We took c=1 and RAM=1 but used the other parameter values listed in the "THIN LEO" column of table 1.)

In both equations (10) and (12), the dominant contribution is made by the smaller of the two currents, ion and electron. In both LEO and GEO the second term in the denominator is dominant because the ion current is the smaller of the two.

It should be noted that if we had included photoelectron contributions:

(a) the photoelectrons (of energy of the order of volts) would readily escape from the negative section but not from the positive section, and

(b) the photoelectron current density escaping from the negative section can be comparable in magnitude with the plasma electron current density on the positive section.

Hence the array would float with roughly equal positive and negative sections. Moreover, the sheath would be thin rather than thick because of the photoelectrons. Thus, the average power loss in GEO (without wake effects) would be of the order of $j_{eo}V$, or 0.1 watt/m^2.

STRUCTURE OF SHEATH IN GEO.

NUMERICAL RESULTS OF COMPUTER CODE "PANEL"

In this section we adopt the linear surface voltage distribution given analytically by the thick-sheath limit (the "THICK SHEATH" diagram in figure 2), and describe the computational approach used and results obtained by the computer code PANEL. Thus, the panel appears as in figure 3, namely, a rectangular plate, with the voltage varying linearly in one direction and constant in the other direction. The voltage runs from -34.7 kv at the negative end to +5.3 kv at the positive end. The 0-kv position is at 0.868 of the panel length. (Since the field is a solution of Laplace's equation, all lengths scale with the length of the panel.)

While the panel voltage configuration has been chosen on the basis of an approximate analysis, the calculation of the field structure requires a numerical technique. A grid method is used, whereby the panel is discretized by a collection of grid points, at which the panel potentials are defined.

Figure 4 shows the panel defined as a section of the x-y plane, in 3-dimensional cartesian x-y-z space. Grid intervals Δx and Δy are chosen, as shown in the figure, but not necessarily uniform. Particle fluxes are calculated at points on the panel by computationally following reversed trajectories to determine their origin. (This "inside-out" method was developed in 1964

(ref. 4) for efficient calculations in steady-state 3-dimensional sheath problems.) Figure 4 shows schematically two possible types of trajectory contributions to a point on the panel; in one example the trajectory comes from the ambient plasma at infinity, while in the other the trajectory comes from another point on the panel (e.g., a secondary or photoelectron). The type of trajectory which actually occurs, for a given incident velocity vector, can only be determined by numerical computation.

In a self-consistent calculation of the floating configuration, the fluxes of ions and electrons at the array points are computed, and the array potentials are adjusted (maintaining fixed relative potential differences) until there is global current balance. Power leakage is calculated by integrating the product of local net current density times local potential over the surface of the array.

The field in the space around the panel is represented by a large grid in 3-dimensional x-y-z space. This is used to calculate forces along trajectories by interpolation between grid points where the potentials are defined. In figure 5 the coarsest possible grid is shown, with only 32 grid points. The panel is represented by the shaded area between 4 grid points. In an actual problem orders of magnitude more points are used, both in space and on the panel. For example, the panel in figure 4 is represented by a 6x7 surface grid of 42 points. This should be embedded in a spatial grid of 1000 to 10000 grid points. About 3000 points were used to obtain the results discussed below.

The numerical field solution is obtained by replacing Laplace's equation by a set of linear algebraic equations, one for each unknown potential. One of the boundary conditions is that the potentials satisfy the prescribed panel surface-potential distribution (shown in figure 3 resulting from the thick-sheath analysis). The other condition is that the potential vanish at infinity. On the outer boundaries of the grid the potential satisfies a suitable relationship between its value and its gradient. The above procedures are outlined in reference 2 and are implemented, for example, in reference 8 for a spacecraft model in r-z geometry.

Linear Voltage Distribution

The field solution for a linearly distributed array in a hydrogen plasma is displayed in figure 6 in the form of a set of equipotential contours. The equipotentials are divided into negative and positive sets, with the zero-potential (space potential) contour tightly enclosing the positive end. Thus, all the positive contours are contained within this small contour. The negative contours have expanded to the right, "engulfing" the positive set and creating a negative saddle point (potential barrier for electrons) at about an array length L to the right of the right end of the array. This happens because the array has a net negative charge. The barrier, of height 2.1 kv, will exclude all electrons with energies less than this. Hence, if the electron temperature is less than 2 kev, the position of zero potential is moved to the left, toward the midpoint (at L/2). If the zero potential were at the midpoint, the negative and positive contours would be symmetric and the potential distribution would be dipole-like.

The solution displayed in figure 6 is the Laplace field. Solutions were also obtained for finite sheath thickness by the assumption of linearized space charge. This leads to a Helmholtz equation with a Debye-length-like parameter (refs. 15-16), whose solutions are 3-D generalizations of the well-known Debye potential. This parameter was assigned successively smaller values, representing a set of solutions (not shown) for diminishing Debye length. With decreasing Debye length, the above potential barrier becomes smaller and is "pulled in" toward the edge of the array.

Alternating Voltages - Overlapping Sheaths

Figure 7 illustrates a panel with alternating strips of zero volts and one kilovolt. This case can represent exposed connections on the backside of an array. It was run to determine the effects of "overlapping sheaths," that is, the effect on the current-voltage characteristic at a point on the surface due to a different potential maintained nearby. For one-volt ions and electrons, it was found that on the zero-volt surfaces the low-energy ions (repelled particles) were excluded (by potential barriers) because of the adjacent +1-kv surfaces, while the electron fluxes (attracted particles) had essentially their random-thermal values. On the 1-kv surfaces, the ion and electron fluxes were essentially the same as for a flat surface entirely at 1 kv, namely, slightly less than half of the ideal Langmuir value due to excluded trajectories for the electrons and the Boltzmann factor for the ions.

Figure 8 displays the equipotential contours for the field solution corresponding to the alternating strips of figure 7, including three saddle points associated with each of the three zero-volt strips. The figure is symmetric about the panel center and is drawn only for the right half. The sizes of the potential barriers, 320 volts and 93 volts, show why the repelled low-energy particles were excluded from the zero-volt strips. If there were infinitely many strips, periodically spaced, the saddle points would also be periodically spaced and centered above the zero-potential strips.

The alternating voltage configuration on the array was assumed. Its floating configuration was not determined. This would require a numerical self-consistent solution because of the potential barriers.

This paper has benefited from the author's discussions with James G. Laframboise.

REFERENCES

1. Parker, L.W.: Differential Charging and Sheath Asymmetry of Nonconducting Spacecraft Due to Plasma Flows. J. Geophys. Res., vol. 83, no. A10, Oct. 1978, p. 4873.

2. Parker, L.W.: Power Loss Calculation for High-Voltage Solar Arrays. Computer Method in Three-Dimensional Space (PANEL). Lee W. Parker, Inc. Report, Feb. 1977.

3. Whipple, E.C., Jr.: Observation of Photoelectrons and Secondary Electrons Reflected from a Potential Barrier in the Vicinity of ATS 6. J. Geophys. Res., vol. 81, 1976, p. 715.

4. Parker, L.W.: Numerical Methods for Computing the Density of a Rarefied Gas About a Moving Object. Allied Res. Assoc. Report AFCRL-64-193, Mar. 1964.

5. Adamo, R.C.; and Nanevicz, J.E.: Effects of Illumination on the Conductivity Properties of Spacecraft Insulating Materials. Stanford Res. Inst. Report NASA CR-135201, July 1977; Coffey, H.T.; Nanevicz, J.E.; and Adamo, R.C.: Photoconductivity of High-Voltage Space Insulating Materials. Stanford Res. Inst. Report, Oct. 1975.

6. Parker, L.W.: Theory of Electron Emission Effects in Symmetric Probe and Spacecraft Sheaths. Lee W. Parker, Inc. Report AFGL-TR-76-0294, Sept. 1976.

7. Grard, R.J.L. (Ed.): Photon and Particle Interactions with Surfaces in Space. D. Reidel, Hingham, Mass., 1973.

8. Parker, L.W.: Calculation of Sheath and Wake Structure About a Pillbox-Shaped Spacecraft in a Flowing Plasma, in Proceedings of the Spacecraft Charging Technology Conference, Report AFGL-TR-77-0051/NASA TMX-73537, Pike, C.P. and Lovell, R.R., Eds., Feb. 1977, p. 331.

9. Parker, L.W.; and Whipple, E.C., Jr.: Theory of a Satellite Electrostatic Probe. Ann. Phys., vol. 44, no. 1, 1967, p. 126.

10. Child, C.D.: Phys. Rev., vol. 32, 1911, p. 492; (see Cobine, J.D.: Gaseous Conductors. Dover, New York, 1958, Eq. 6.9); Langmuir, I.: Phys. Rev., vol. 2, 1913, p. 450 (see ref. 11).

11. Langmuir, I.; and Blodgett, K.B.: Currents Limited by Space Charge Between Concentric Spheres. Phys. Rev., vol. 24, 1924, p. 49.

12. Liemohn, H.B.: Electrical Charging of Shuttle Orbiter. IEEE Trans. Plasma Sci., vol. PS-4, no. 4, Dec. 1976, p. 229.

13. Laframboise, J.G.; and Parker, L.W.: Probe Design for Orbit-Limited Current Collection. Phys. Fluids, vol. 16, no. 5, 1973, p. 629.

14. Parker, L.W.; and Laframboise, J.G.: Multi-Electrode Plasma Probe for Orbit-Limited-Current Measurements. II. Numerical Verification. Phys. Fluids, vol. 21, no. 4, 1978, p. 588.

15. Parker, L.W.: Computation of Ion Collection by a Large Rocket-Mounted Mass-Spectrometer Plate at a Large Drawing-In Potential. Mt. Auburn Res. Assoc. Report AFCRL-72-0524, Sept. 1972.

16. Parker, L.W.: Computer Solutions in Electrostatic Probe Theory, Part II. Two-Electrode Systems in r,z Geometry. Mt. Auburn Res. Assoc. Report AFAL-TR-72-222, Apr. 1973.

Table 1.

SHEATH THICKNESS, LENGTHS, AND VOLTAGES OF POSITIVE AND NEGATIVE SECTIONS OF A 40-kv ARRAY OF LENGTH 1 km

	THIN LEO (O^+ ions)	THIN GEO (H^+ ions)	THICK GEO (H^+ ions)
M = ion Mach number	6.4	0	0
RAM = ram current factor	23	1	1
L_2(m) = length of positive section	117	23	132
L_1(m) = length of negative section	883	977	868
V_2(v) = positive-end voltage	+4700	+900	+5300
V_1(v) = negative-end voltage	-35300	-39100	-34700
$n_0(cm^{-3})$ = ambient plasma density	10^5	1	1
T(ev) = ambient plasma temperature	0.1	10^4	10^4
S_2(m) = sheath thickness at positive end	30	150	∞
S_1(m) = sheath thickness at negative end	28	2600	∞

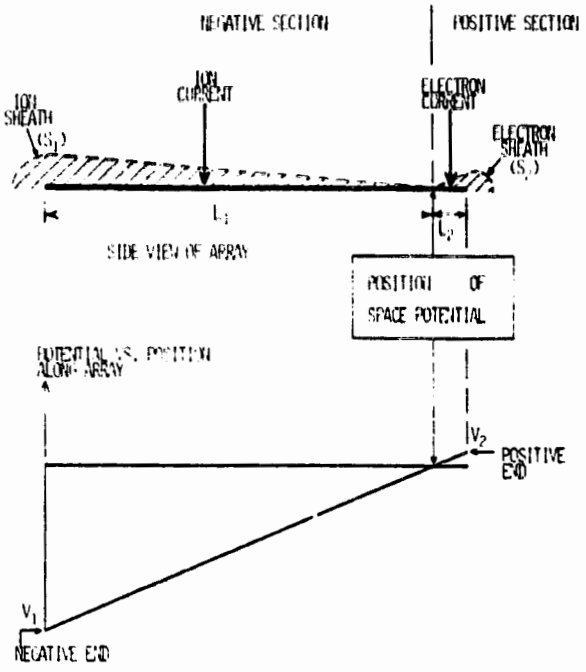

Figure 1. - Linear voltage variations in rectangular sheath panels.

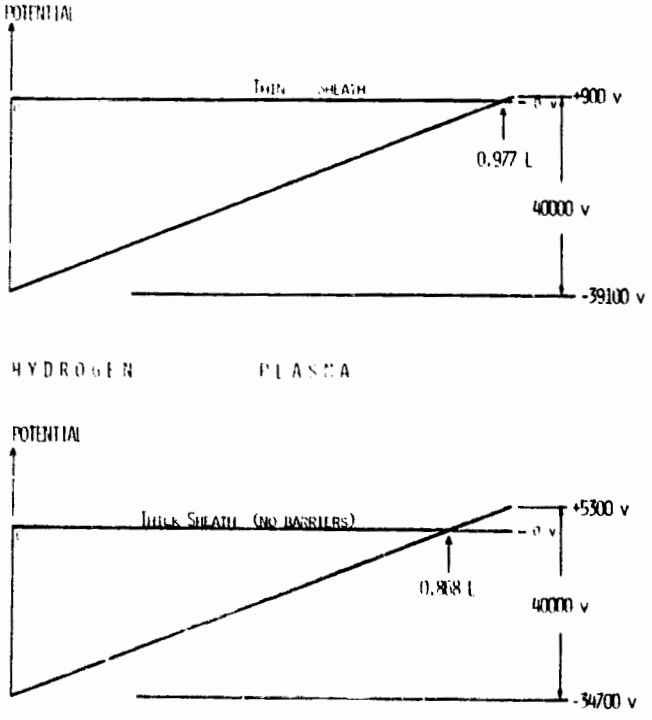

Figure 2. - Linear floating voltage configurations - thin- and thick-sheath limits in hydrogen plasma.

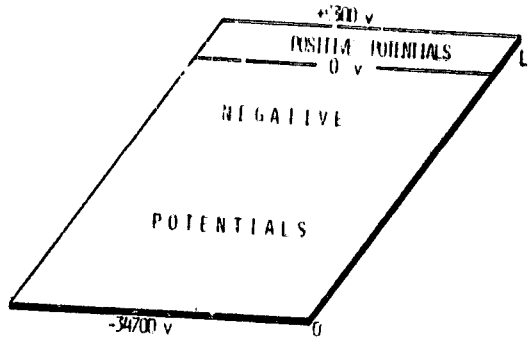

Figure 3. - Model for array sheath calculation - thick-sheath limit in hydrogen plasma.

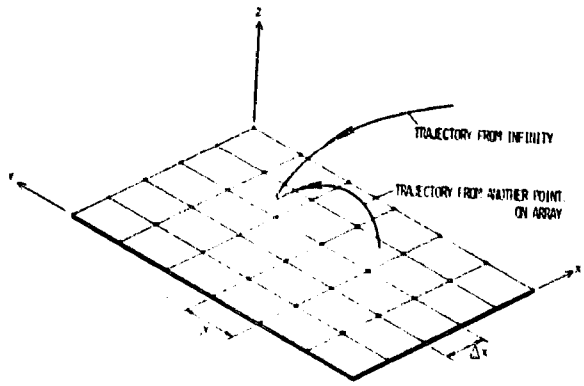

Figure 4. - Computational model for array panel.

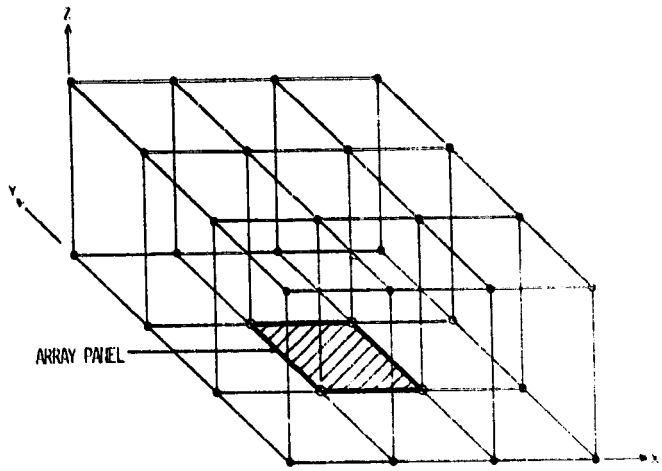

Figure 5. - Computational grid for array sheath calculation.

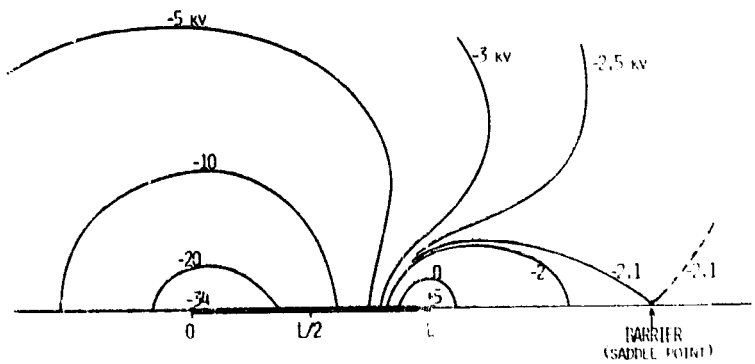

Figure 6. - Equipotential contours (in kilovolts) for sheath of floating linear array.

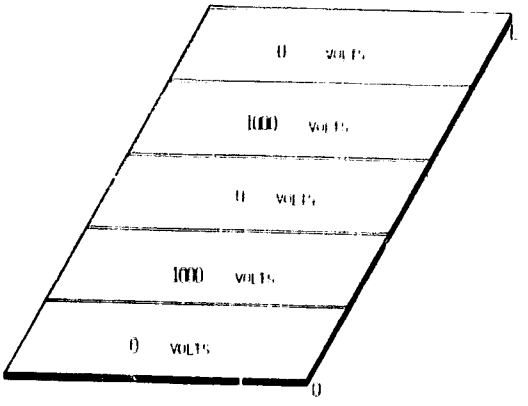

Figure 7. - Model for overlapping sheaths of alternating high- and low-voltage areas.

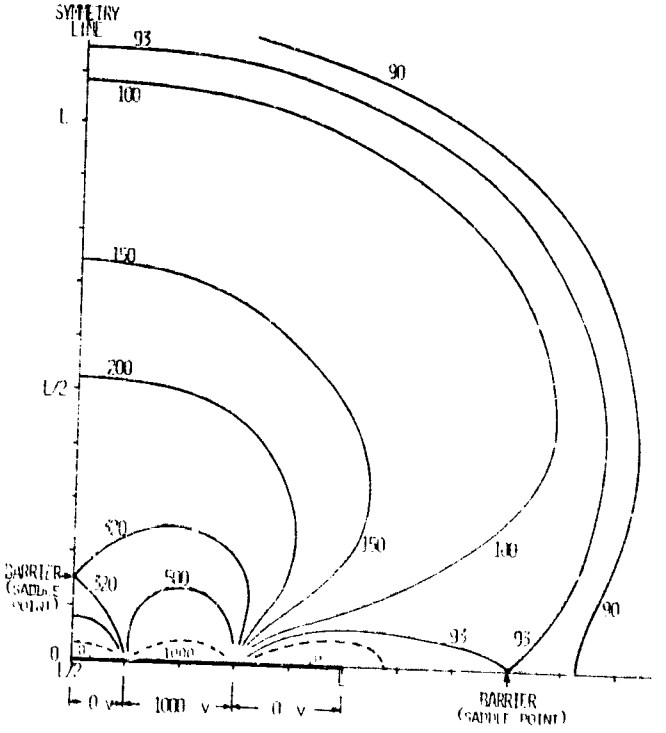

Figure 8. - Equipotential contours (in volts) for overlapping sheaths of alternating high- and low-voltage areas.